Published in final edited form as:
Arterioscler Thromb Vasc Biol. 2012 May ; 32(5): 1132–1141. doi:10.1161/ATVBAHA.111.244061.

Progression from obesity to metabolic syndrome is associated with altered myocardial autophagy and apoptosis

Zi-Lun Li, MD, PhD[1,2], **John R. Woollard**[1], **Behzad Ebrahimi, PhD**[1], **John A. Crane**[1], **Kyra L. Jordan**[1], **Amir Lerman, MD**[3], **Shen-Ming Wang, MD, PhD**[2], and **Lilach O. Lerman, MD, PhD**[1,3]

[1]Division of Nephrology and Hypertension, Mayo Clinic, Rochester, MN

[2]Division of Vascular Surgery, the First Affiliated Hospital, Sun Yat-sen University, Guangzhou, China

[3]Division of Cardiovascular Diseases, Mayo Clinic, Rochester, MN

Abstract

Objective—Transition from obesity to metabolic-syndrome (MetS) promotes cardiovascular diseases, but the underlying cardiac pathophysiological mechanisms are incompletely understood. We tested the hypothesis that development of insulin resistance (IR) and MetS is associated with impaired myocardial cellular turnover.

Methods and results—MetS-prone Ossabaw pigs were randomized to 10 weeks of standard chow (lean), or to 10 (obese) or 14 (MetS) weeks of atherogenic diet (n=6 each). Cardiac structure, function, and myocardial oxygenation were assessed by multidetector computed-tomography and Blood-Oxygen-Level-Dependent (BOLD)-magnetic resonance imaging (MRI), the microcirculation with micro-computed-tomography, and injury mechanisms by immunoblotting and histology. Both obese and MetS showed obesity and dyslipidemia, while only MetS showed IR. Cardiac output and myocardial perfusion increased only in MetS, yet BOLD-MRI showed hypoxia. Inflammation, oxidative stress, mitochondrial dysfunction, and fibrosis also increased in both obese and MetS, but more pronouncedly in MetS. Furthermore, autophagy in MetS was decreased and accompanied by marked apoptosis.

Conclusions—Development of IR characterizing a transition from obesity to MetS is associated with progressive changes of myocardial autophagy, apoptosis, inflammation, mitochondrial dysfunction, and fibrosis. Restoring myocardial cellular turnover may represent a novel therapeutic target for preserving myocardial structure and function in obesity and MetS.

Keywords

obesity; metabolic-syndrome; cardiac function; autophagy; inflammation

Obesity has reached epidemic proportions and risen to 34% among adults in the United States.[1] Obesity is related to increased prevalence of type 2 diabetes, with excess adiposity

Correspondence: Lilach O. Lerman, MD, PhD., Division of Nephrology and Hypertension, Mayo Clinic, 200 First Street SW, Rochester, MN 55905. lerman.lilach@mayo.edu (L.O. Lerman), Phone: (507)-266-9376, Fax: (507)-266-9316.

Disclosures
None.

being a critical contributor to the development of insulin resistance (IR).[2] The incidence of metabolic syndrome (MetS), a cluster of cardiovascular risk factors with obesity and IR as major components, increases with the severity of obesity and reaches 50% in severely obese youngsters.[3] MetS is associated with increased cardiovascular morbidity and mortality,[4] partially related to left ventricular (LV) diastolic dysfunction.[5]

One of the mechanisms by which development of IR in obese subjects might exacerbate cardiac injury is inflammation, as macrophages that infiltrate adipose tissue in obesity play a pivotal role in obesity and IR.[6] Furthermore, myocardial inflammation, evidenced by increases in cardiac macrophages and cytokines in obesity, suppresses myocardial glucose metabolism[7] and increases fibrosis in obesity-induced MetS.[8]

Normal myocardial cellular turnover depends on adequate disposal of damaged proteins and organelles (autophagy) or cells (apoptosis). Autophagy, a critical catabolic process through which damaged cytoplasmic components are degraded and recycled, controls cellular contents quality and homeostasis.[9] Increasing evidence indicates that cardiovascular diseases might be associated with maladaptation of autophagy.[10, 11] While autophagic activation is a cellular response to starvation, autophagy is also impaired in hypercholesterolemia[12] and obesity[13], which may lead to accumulation of damaged mitochondria[14] in muscle and defective insulin signaling in the liver.[15] Conversely, myocardial autophagy is activated in nonobese mice with fructose-induced IR.[16] Yet, whether myocardial autophagic activity is altered by the microenvironment characterizing obesity and IR remains largely unknown.

Therefore, this study aimed to test the hypothesis that transition from obesity to MetS, as reflected by development of IR, is characterized by impaired myocardial autophagy, in association with inflammation and fibrosis. We studied both *in-vivo* and *ex-vivo* hearts of Ossabaw pigs, a unique large animal model that progressively gains components[17] mimicking human MetS.

Methods

The study was approved by the Institutional Animal Care and Use Committee. Littermate 3-months-old Ossabaw pigs (Swine Resource, Indiana University) started a 10-week standard chow (lean), or 10 (obese) or 14 (MetS) weeks of atherogenic diet (5B4L; Purina Test Diet, Richmond, Indiana)[18] (n=6 each group). Blood and urine samples under fasting conditions were subsequently collected, and the pigs studied with Magnetic Resonance Imaging (MRI, for myocardial oxygenation) followed by multidetector computed-tomography (MDCT, for cardiac structure, function, and myocardial perfusion) 2 days later. Three days following the completion of *in-vivo* studies, pigs were euthanized with pentobarbital-sodium (100mg/kg IV, Sleepaway®, Fort Dodge Laboratories, Fort Dodge, Iowa), hearts were removed, immediately shock-frozen in liquid nitrogen and stored at −80°C, preserved in formalin, or prepared for micro-CT studies. Myocardial autophagy, apoptosis, oxidative stress, inflammation, lipid accumulation, microvascular (MV) architecture, and fibrosis were then determined.

Systemic measurements

Blood pressure and heart rate were recorded with an intra-arterial catheter during the MDCT study. Rate-pressure product (RPP), an index of myocardial oxygen consumption, was calculated by heart rate×systolic blood pressure×10^{-2}. Levels of plasma renin activity (PRA), endothelin (ET)-1, tumor-necrosis-factor-α (TNF-α), and monocyte-chemoattractant-protein (MCP)-1 were tested as previously described,[19, 20] and total cholesterol, triglycerides (TG), low-density lipoprotein (LDL), and high-density lipoprotein (HDL) by

standard procedures. Intravenous glucose-tolerance test (IVGTT) was performed before CT scanning,[17] and the homeostasis model assessment insulin resistance (HOMA-IR) index (fasting plasma glucose × fasting plasma insulin/22.5) used as an index of IR.[19] Systemic oxidative stress was evaluated by plasma levels of oxidized LDL (Ox-LDL, Alpco Diagnostics, Windham, NH) and 8-isoprostanes (EIA, Cayman Chemical, Ann-Arbor, MI).[18]

In-vivo studies

For each *in-vivo* study animals were weighed, induced with IM Telazol (5mg/kg) and xylazine (2 mg/kg), intubated, and ventilated with room air.

Imaging—Blood Oxygen Level-Dependent (BOLD)-MRI was used to acquire myocardial oxygenation data (BOLD index, R_2*), subsequently analyzed using MATLAB 7.10 (The MathWorks Inc, Natick, MA), as we have shown.[21] MDCT studies performed 2 days after MRI evaluated cardiac structure and function, as shown previously.[22] LV muscle mass, systolic function, early (E) and late (A) LV filling rates were calculated, as well as myocardial perfusion and MV permeability index before and during adenosine infusion, as we described.[20, 22, 23] Intra-abdominal adipose tissue measured using MDCT was expressed as volume and fraction.[18, 19] See Supplemental data for detail.

In-vitro studies

Myocardial hypoxia was evaluated by Western-blotting of hypoxia-inducible factor (HIF)-1α, and angiogenic activity by vascular endothelial growth factor (VEGF) and its receptor Flk-1. Myocardial redox status was evaluated by in-situ production of superoxide anion, detected by dihydroethidium (DHE) (Sigma, 20 uM/L), and by protein expression of the P47, P67, and GP91 subunits of NAD(P)H oxidase, and superoxide dismutase (SOD)-1. Inflammation was investigated by staining for macrophage markers CD163 and CD8, and by protein expression of the activated T-lymphocyte marker CD134, interleukin (IL)-6, MCP-1, its receptor C-C motif receptor (CCR)-2, and TNF-α. Mitochondrial biogenesis and energy metabolism were assessed by protein expression of sirtuin-1, peroxisome proliferator-activated receptor-gamma-coactivator 1- α (PGC-1α), ATP synthase mitochondrial-F1-complex-assembly-factor-1 (ATPAF1), uncoupling protein-2 (UCP2), and creatine transporter-1 (CT1). Fibrosis was studied by Sirius-red and trichrome staining, as well as protein expression of matrix-metalloproteinase (MMP)-2, tissue inhibitor of metalloproteinase (TIMP)-1, plasminogen-activator inhibitor (PAI)-1 and transforming growth-factor (TGF)-β1. Autophagy was assessed by protein expression of unc-51-like kinase-1, Beclin-1, autophagy-related gene (Atg)-12, microtubule-associated protein-1 light-chain (LC)-3, phospho-AMP-activated protein kinase (p-AMPK), and mammalian target of rapamycin (mTOR). Apoptosis was evaluated by Terminal deoxynucleotidyl transferase dUTP nick end labeling (TUNEL, green) and cleaved (active) caspase-3 (red) double-staining, as well as expression of CCAAT/enhancer binding protein (C/EBP) homologous protein (CHOP) and phosphorylated signal-transducer and activator of transcription (STAT)-3. For Western-blotting, GAPDH was used as loading control, except for pro-MMP-2 and total STAT-3 for corresponding proteins. LC3 conversion was evaluated by LC3 II-to-LC3 I ratio. LV triglyceride levels were quantified as recently described.[18] See Supplemental data for detail.

Micro-CT—The left-anterior-descending coronary artery was perfused with a radio-opaque polymer, and a transmural portion of the LV myocardium then scanned as previously described.[22, 24, 25] Microvessels were classified using Analyze™ as small (diameters 20–200 μm), medium (201–300 μm), or large (301–500 μm). See Supplemental data for detail.

Histology—Staining performed on 5-μm-thick myocardial cross-sections was semiautomatically quantified by a computer-aided image analysis program (MetaMorph®, Molecular Devices, Sunnyvale, CA).[22] Staining in 10 random fields was quantified and expressed as fraction of surface area or of total cells stained with DAPI.

Effects of obesity and IR on myocardial tissue pathomechanisms in domestic pigs

To further confirm that development of IR rather than duration of obesity altered myocardial autophagy and apoptosis, 3 additional groups of domestic farm pigs were studied: normal (standard chow, n=6), obese domestic (obese-D) (high-fat diet, n=6),[19] and IR domestic (IR-D) pigs (atherogenic diet, n=2), all for 12 weeks.[18] These models (on a different background than the MetS-prone Ossabaw model) were achieved using different diets that we have found to induce obesity[19] in domestic pigs, and the same atherogenic diet used for the Ossabaw model, which led to mild but significant IR in the domestic swine. After 12 weeks of diet, representative in-vivo and in-vitro studies were performed.

Statistical analysis

Continuous data are expressed as mean±SEM. Comparisons within groups were performed using the paired Student t-test and among groups using ANOVA and unpaired t-test with Bonferroni correction. $p \leq 0.05$ was considered statistically significant.

Results

Systemic characteristics

Body weight and visceral fat accumulation were greater in obese Ossabaw pigs than lean, and greater yet in MetS (Table 1). Compared with lean pigs, total cholesterol, LDL, HDL, and LDL/HDL ratio were similarly elevated in both obese and MetS pigs, while serum triglycerides tended to be higher (p=0.09) in MetS than lean pigs. Blood pressure, heart rate, RPP (Table 1), PRA, ET-1, TNF-α, and MCP-1 (data not shown) remained unchanged. Basal insulin levels tended to increase in obese compared with lean pigs (p=0.06), but were significantly higher in MetS; basal glucose levels in MetS increased compared with obese and tended to increase compared with lean pigs (p=0.07), and their HOMA-IR were elevated compared with both groups (Fig.1A). Compared with lean, 8-epi-isoprostane increased in both obese and MetS pigs, while ox-LDL increased only in MetS.

Cardiac hemodynamics and function

The relatively low heart rate observed might have been attributable to the effect of xylazine anesthesia. LV muscle mass increased in obese pigs and tended to further increase (p=0.08 vs. obese) in MetS, but this elevation disappeared after being indexed to body weight. Further, LV wall thickness represented by wall area showed no difference among the groups during either systole or diastole. E/A was higher in the obese and MetS groups, suggesting LV diastolic dysfunction with restrictive filling. LV end-diastolic volume (EDV) was larger in MetS pigs, while end-systolic volume (ESV) remained unchanged. EDV and ESV of left atrium were not different among the groups (Supplemental Table I). Stroke volume, cardiac output, and ejection fraction were higher only in MetS compared with lean pigs, whereas cardiac index remained unchanged. Basal CT-derived myocardial perfusion increased in MetS, but only lean pigs showed a significant response to adenosine, which tended to be attenuated in obese (p=0.06) compared with lean pigs, and was significantly blunted in MetS (Table 1). Contrarily, the permeability index in MetS significantly increased in response to adenosine, suggesting impaired myocardial microvascular integrity.

Myocardial oxygenation

Basal myocardial R_2* values were higher in MetS compared with lean and obese pigs (Fig. 1B–D), suggesting myocardial hypoxia. R_2* values strongly tended to decrease (possibly due to substantial variation) in lean pigs in response to adenosine (p=0.06 vs. baseline), but failed to decrease in either obese (p=0.15 vs. baseline) or MetS, suggesting MV dysfunction (Fig. 1E–G). HIF-α (Fig. 1N) tended to increase (p=0.07) in MetS compared with the lean group.

Cardiac adiposity

Pericardial fat was markedly and similarly elevated in obese and MetS pigs (Fig. 1H–J), and Oil-Red-O staining increased (Fig. 1K–M). Myocardial tissue triglyceride levels were also higher in obese and MetS (Fig. 1S).

Microcirculation

The density of subendocardial microvessels (20–200 μm) tended to increase (p=0.08) in obese hearts, and increased significantly in MetS (Fig. 2A–D), while subepicardial MV density was unchanged (data not shown). MV tortuosity, an index of angiogenesis and vascular immaturity, increased in both obese and MetS pigs (Fig. 2E). Interestingly, protein expression of VEGF increased in obese, but declined to normal levels in MetS pigs. Conversely, protein expression of FLK-1 was upregulated only in MetS pigs (Fig. 2F–G), possibly as a compensatory mechanism.

Inflammation and oxidative stress

Infiltration of CD163+ macrophage and CD8+ T-cells increased only in MetS compared to lean and obese, as was the expression of CD134 (Fig. 3). Myocardial expression of IL-6 increased in obese and further enhanced in MetS, whereas CCR2 and TNF-α increased only in MetS and MCP-1 remained unaltered. Superoxide anion production and SOD1 expression increased in both the obese and MetS groups (Fig. 3), while myocardial expression of the NAD(P)H oxidase subunits was magnified in MetS compared to obese pigs (Fig. 3).

Mitochondrial function and energy metabolism

Myocardial expression of SIRT1 and ATPAF1 decreased in MetS compared with both lean and obese pigs. PGC-1α similarly decreased in obese and MetS pigs, while UCP decreased in obese and further decreased in MetS. CT1 expression increased in MetS compared with lean and obese pigs (Fig. 4). Collectively, these suggest impaired mitochondrial function and energy metabolism.

Myocardial fibrosis

The level of total collagen (Sirius red staining) was elevated in obese and further increased in MetS pigs (Fig. 4). Trichrome staining showed that fibrosis tended to increase (p=0.06) in obese, and increased markedly in MetS compared with lean pigs. Protein expression of PAI-1 and MMP-2 was also upregulated in MetS compared with obese pigs, whereas TGF-β and TIMP-1 were unchanged (Fig. 4).

Autophagy and apoptosis

Protein expression of ULK1 was lower in MetS compared with obese pigs. Conjugated Atg12-Atg5 was elevated in both obese and MetS, whereas decreases in Beclin-1 and LC3 conversion did not reach statistical significance in obese pigs (p=0.06 and 0.08, respectively), but were pronounced in MetS. Expression of mTOR increased markedly in MetS compared with lean pigs (Fig. 5), while p-AMPK remained unchanged. Apoptotic

activity assessed by TUNEL and caspase-3 staining has not reached statistical significance levels in obese pigs (p=0.06 and p=0.09, respectively), but was pronounced in MetS. This was accompanied by elevated protein expression of CHOP in MetS and decreased phospho-STAT-3 in both groups (Fig. 5).

Obesity and IR in domestic swine

Obese-D and IR-D pigs had similarly elevated body weight, while IR only developed in IR-D pigs (Supplemental Table II). IR-D pigs showed greater hyperlipidemia compared with obese pigs, but their intra-abdominal fat was not increased compared with normal pigs, and was lower than in obese pigs. Plasma triglycerides in IR-D pigs were lower than normal and tended to be lower than in obese-D pigs (p=0.07). In vitro studies showed that obese-D and IR-D pigs had similar inflammation and oxidative stress (CCR2 and P47, respectively). IR-D pigs showed increased fibrotic activity reflected by increased expression of active MMP2, and presented mitochondrial dysfunction (decreased PGC-1α and UCP2 expression). Obese-D pigs showed depressed autophagy (increased mTOR), which was exacerbated in IR pigs, as demonstrated by an additional tendency (p=0.088) of Atg12-Atg5 to decline. Further, Obese-D pigs showed slightly increased apoptosis, which was magnified in IR-D, as shown by TUNEL and cleaved Caspase-3 staining (Supplemental Figure I). Taken together, development of IR exacerbated myocardial autophagy and apoptosis in domestic pigs with IR.

Discussion

This study shows that the early phase of visceral obesity is characterized by myocardial adiposity, accompanied by diastolic dysfunction, mild inflammation, oxidative stress, and mitochondrial dysfunction. Subsequent development of IR magnifies MV proliferation and dysfunction, and aggravates myocardial inflammation, oxidative stress, mitochondrial dysfunction, and fibrosis. Furthermore, we demonstrated in several different swine models that IR might suppress autophagy and trigger apoptosis, suggesting attenuated defense mechanisms leading to cell death.

Obesity has become pandemic that causes devastating health problems, with excess fat accumulation being a major contributor to the development of IR and a transition to MetS.[2] However, the structural and functional myocardial alterations that characterize this transition are poorly understood. In this study we took advantage of a unique MetS-prone swine model and state-of-the-art imaging technologies to reveal underlying pathomechanisms of myocardial injury in obesity and its transition to MetS. After 10 weeks of atherogenic diet, the Ossabaw pigs developed central obesity and pericardial fat. Extending the atherogenic diet for another 4 weeks invoked marked IR, expanding the cluster of risk factors typical for MetS, including obesity, dyslipidemia, and IR.

Importantly, IR is considered a critical factor linking visceral adiposity to cardiovascular risk. While TNF-α and MCP-1 have been implicated in obesity-induced IR,[26] the unchanged levels that we observed argue against a major role of these inflammatory factors in our swine model. Conversely, an increase in systemic oxidative stress in obese pigs that was exacerbated in MetS paralleled the development of IR, consistent with accumulating evidence implicating oxidative stress in contributing to development of IR.[27] In some models, appearance of metabolic and cardiovascular components tracks together during development of MetS,[28] whereas in our model obesity preceded IR, and MetS developed as obesity worsened.

The risk imposed by obesity for increased cardiovascular morbidity may involve several mechanisms. Excess adipose tissue with high metabolic activity increases total blood

volume and cardiac output, which may eventually lead to LV dilation, increased wall stress, compensatory hypertrophy, and diastolic dysfunction.[29] Thus, augmented systolic function in MetS pigs might be attributed to their higher body weights. An E/A ratio≥2 in obese and MetS pigs may imply LV diastolic dysfunction of restrictive filling pattern, as observed in obese rats.[30] Accumulation of pericardial fat pads may increase ventricular stiffness and restrict filling[31], and excessive cardiomyocytes lipid deposits (cardiac steatosis) may cause contractile dysfunction[32]. The similar cardiac diastolic dysfunction in obesity and MetS was accompanied by comparable myocardial fat accumulation, although the increased EDV in MetS may suggest greater cardiac dilation. The association between lipids and myocardial dysfunction is likely mediated by toxic fatty-acid intermediates, which increase oxidative stress and apoptosis.[33] Pertinently, development of IR instigates a vicious cycle of increased cardiomyocytes fatty-acid uptake, oxidative-stress, and triglycerides deposit.[33]

Impaired myocardial metabolism is associated with diastolic dysfunction in diabetes.[34] Indeed, we observed in obese pigs impaired mitochondrial function and energy metabolism, which was exacerbated in MetS. Accordingly, SIRT1 is downregulated in MetS, particularly in IR compared with insulin-sensitive subjects.[35] We found lower level of SIRT1 in MetS but not in obese pigs, indicating a link between IR and depressed SIRT1. Importantly, SIRT1 activates PGC-1α, a master regulator of mitochondrial biogenesis and energy metabolism.[36] Downregulation of SIRT1 and PGC-1α suggest compromised mitochondrial biogenesis in MetS pigs. Of note, PGC-1α was also inhibited in obese pigs. Reduction of PGC-1α is associated with a conversion from fatty acid oxidation to glycolytic metabolism under stress,[36] possibly constituting a compensatory mechanism in obesity, which IR impairs in MetS.[37] Furthermore, PGC-1α-deficient hearts show decreased levels of ATP and phosphocreatine.[38] Indeed, decreased activity of ATP synthase (downregulated ATPAF1) was only found in MetS pigs, likely implying decreased formation of ATP, while CT1 upregulation in MetS was possibly compensatory to insufficient phosphocreatine, given a feedback-loop of CT1.[39] Thus, decreased myocardial oxygenation detected by BOLD-MRI after development of IR might be secondary to impaired glucose utilization, as oxygen consumption remained unchanged. Nonetheless, decreased hemoglobin saturation may contribute to lower resting R2*, as does elevated capillary volume (increasing deoxygenated blood availability). Furthermore, macrophages and cytokines like IL-6 detected in MetS may blunt myocardial glucose metabolism.[7] This is in agreement with evidence from Framingham Offspring Study that MetS requires IR to increase risk for cardiovascular disease.[40]

Increased myocardial fibrosis and stiffness observed in obese and MetS pigs may also contribute to LV diastolic dysfunction, as collagen and fibrosis determine tissue compliance, which is inversely associated with LV diastolic function.[41,42] While cardiac TGF-β expression was not different among the groups, PAI-1 was upregulated in MetS, likely secondary to IR.[43] The increased expression of MMP-2 also implicates abnormal matrix turnover in the fibrogenesis.

We found enhanced myocardial angiogenesis in obese and MetS pigs, as observed in kidneys of obese pigs[18] and rats[44]. Indeed, hypercholesterolemia per se induces myocardial neovascularization in domestic pigs, associated with myocardial ischemia[24], inflammation, and oxidative stress[25]. Notably, MV proliferation increased selectively in the relatively vulnerable subendocardium. Interestingly, myocardial perfusion was elevated in MetS, likely because of their increased systolic function. However, newly formed vessels may not function properly because of their impaired integrity, suggested by enhanced permeability but blunted perfusion response to adenosine in MetS. Furthermore, permeable vessels permit extravasation of inflammatory cells releasing inflammatory mediators, which were all increased in MetS. Notably, myocardial expression of VEGF initially increased in obese

pigs but subsequently fell in MetS, yet microvascular density showed no difference between them, likely due to increased expression in MetS of the FLK-1 receptor, which mediates the angiogenic effects of VEGF.

Our study shows for the first time that in Ossabaw swine excessive nutrition progressively inhibits cardiac autophagic activity, which might be at least partially responsible for myocardial injury. The transition from obesity to MetS in our study prominently involved attenuated autophagy, which may contribute to development of IR.[13] Although cardiac conjugated Atg12-Atg5 expression increased in obese and MetS, as also found in defective hepatic autophagy in obesity,[13] ULK1, Beclin-1, and LC3 conversion all decreased in MetS, suggesting inhibited formation of nascent and mature autophagosomes. Furthermore, upregulation of the autophagy inhibitor mTOR in MetS underscores impairment in autophagy as IR develops. Indeed, SIRT1 can activate autophagy by inhibition of mTOR[45], and its downregulation, linked to IR,[35] may contribute to inhibition of autophagy in MetS. Chronic lipid load[46] and cytokines[47] may blunt autophagy, in line with the myocardial adiposity in obese and MetS pigs and exacerbated inflammation in MetS.

Importantly, inhibition of autophagy may lead to accumulation of damaged cellular components that eventuates in cell death.[48] Impaired mitochondrial biogenesis evidenced by decreased PGC-1α was observed in both obese and MetS. Further, decreased autophagy in MetS compromises autophagic clearance of damaged mitochondria, resulting in their accumulation and thereby apoptosis.[14] Indeed, we found marked apoptosis in the MetS myocardium, accompanied by increased CHOP and decreased p-STAT3 expression. In turn, apoptosis of hepatocytes[49] and adipocytes[50] has been linked to development of IR. Notably, increased apoptosis was observed in early diabetic cardiomyopathy, in which diastolic dysfunction preceded systolic dysfunction.[51] As apoptosis leads to systolic dysfunction, altered survival signaling may be partially responsible for the transition from diastolic to systolic dysfunction in diabetic cardiomyopathy.[51] Indeed, marked myocardial apoptosis was observed after 12 weeks of established diabetes with coexistent impaired LV diastolic and systolic function.[52] Conceivably, apoptosis may represent a mechanism underlying the progression from diastolic dysfunction at early MetS, as suggested in our study, to systolic dysfunction at later stage. Importantly, our observations made in several different pig models underscore the important role of IR underlying this pathophysiology. Thus, suppressed autophagy and increased apoptosis may be critical elements in the cascade of cardiac injury in MetS.

Limitations

The present study design did not afford establishing a causal relationship among the functional and structural variables in obesity and MetS, which are rather complex biologic systems. Indeed, the clinically-relevant swine models of diet-induced obesity and MetS successfully mimicked the complexity of obesity-induced metabolic disorders, and thus allowed us to correlate the dynamic pathophysiological changes in the heart in-vivo and ex-vivo. In addition, autophagy flux is difficult to measure in-vivo, especially in large swine models. We also cannot rule out the possibility that some of the exacerbated cardiac injury in Ossabaw MetS is secondary to more severe or prolonged obesity rather than IR. However, the observation that similar mechanisms were activated in domestic pig models with selectively-induced IR and comparable duration of obesity supports the link between IR, attenuated autophagy, and magnified apoptosis. Hence, our study enabled demonstration of progression of myocardial insult due to obesity and development of IR, and exploring their incremental effects on heart.

In summary, our study demonstrated pathophysiological changes in the heart of several different swine models of experimental obesity and MetS both *in-vivo* and *in-vitro*.

Transition from obesity to MetS and development of IR are associated with impairment of myocardial autophagy, and progressive increase in inflammation, mitochondrial dysfunction, apoptosis, and fibrosis. Maintaining the balance of myocardial organellar and cellular turnover and reducing inflammation may represent novel therapeutic targets for preserving myocardial structure and function in obesity and MetS.

Supplementary Material

Refer to Web version on PubMed Central for supplementary material.

Acknowledgments

Zilun Li is supported by the China Scholarship Council under the authority of the Ministry of Education of the People's Republic of China.

Sources of Funding

This study was partly supported by NIH grants numbers DK73608, HL77131, HL085307 and C06-RR018898.

References

1. Flegal KM, Carroll MD, Ogden CL, Curtin LR. Prevalence and trends in obesity among US adults, 1999–2008. JAMA-J. Am. Med. Assoc. 2010; 303:235–241.
2. Cornier MA, Marshall JA, Hill JO, Maahs DM, Eckel RH. Prevention of overweight/obesity as a strategy to optimize cardiovascular health. Circulation. 2011; 124:840–850. [PubMed: 21844090]
3. Weiss R, Dziura J, Burgert TS, Tamborlane WV, Taksali SE, Yeckel CW, Allen K, Lopes M, Savoye M, Morrison J, Sherwin RS, Caprio S. Obesity and the metabolic syndrome in children and adolescents. N. Engl. J. Med. 2004; 350:2362–2374. [PubMed: 15175438]
4. Isomaa B, Almgren P, Tuomi T, Forsen B, Lahti K, Nissen M, Taskinen MR, Groop L. Cardiovascular morbidity and mortality associated with the metabolic syndrome. Diabetes Care. 2001; 24:683–689. [PubMed: 11315831]
5. de las Fuentes L, Brown AL, Mathews SJ, Waggoner AD, Soto PF, Gropler RJ, Davila-Roman VG. Metabolic syndrome is associated with abnormal left ventricular diastolic function independent of left ventricular mass. Eur. Heart J. 2007; 28:553–559. [PubMed: 17311827]
6. Xu HY, Barnes GT, Yang Q, Tan Q, Yang DS, Chou CJ, Sole J, Nichols A, Ross JS, Tartaglia LA, Chen H. Chronic inflammation in fat plays a crucial role in the development of obesity-related insulin resistance. J. Clin. Invest. 2003; 112:1821–1830. [PubMed: 14679177]
7. Ko HJ, Zhang ZY, Jung DY, Jun JY, Ma ZX, Jones KE, Chan SY, Kim JK. Nutrient stress activates inflammation and reduces glucose metabolism by suppressing amp-activated protein kinase in the heart. Diabetes. 2009; 58:2536–2546. [PubMed: 19690060]
8. Panchal SK, Poudyal H, Iyer A, Nazer R, Alam MA, Diwan V, Kauter K, Sernia C, Campbell F, Ward L, Gobe G, Fenning A, Brown L. High-carbohydrate high-fat diet-induced metabolic syndrome and cardiovascular remodeling in rats. J. Cardiovasc. Pharmacol. 2011; 57:51–64. [PubMed: 20966763]
9. Nemchenko A, Chiong M, Turer A, Lavandero S, Hill JA. Autophagy as a therapeutic target in cardiovascular disease. J Mol Cell Cardiol. 2011; 51:584–593. [PubMed: 21723289]
10. Hein S, Arnon E, Kostin S, Schonburg M, Elsasser A, Polyakova V, Bauer EP, Klovekorn WP, Schaper J. Progression from compensated hypertrophy to failure in the pressure-overloaded human heart - structural deterioration and compensatory mechanisms. Circulation. 2003; 107:984–991. [PubMed: 12600911]
11. Zhu HX, Tannous P, Johnstone JL, Kong YL, Shelton JM, Richardson JA, Lei V, Levine B, Rothermel BA, Hill JA. Cardiac autophagy is a maladaptive response to hemodynamic stress. J. Clin. Invest. 2007; 117:1782–1793. [PubMed: 17607355]

12. Glazer HP, Osipov RM, Clements RT, Sellke FW, Bianchi C. Hypercholesterolemia is associated with hyperactive cardiac mtorc1 and mTORC2 signaling. Cell Cycle. 2009; 8:1738–1746. [PubMed: 19395857]
13. Yang L, Li P, Fu SN, Calay ES, Hotamisligil GS. Defective hepatic autophagy in obesity promotes er stress and causes insulin resistance. Cell Metab. 2010; 11:467–478. [PubMed: 20519119]
14. Menzies KJ, Hood DA. The role of sirt1 in muscle mitochondrial turnover. Mitochondrion. 2011 In press.
15. Zhou LJ, Liu F. Autophagy roles in obesity-induced er stress and adiponectin downregulation in adipocytes. Autophagy. 2010; 6:1196–1197. [PubMed: 20864818]
16. Mellor KM, Bell JR, Young MJ, Ritchie RH, Delbridge LMD. Myocardial autophagy activation and suppressed survival signaling is associated with insulin resistance in fructose-fed mice. J Mol Cell Cardiol. 2011; 50:1035–1043. [PubMed: 21385586]
17. Dyson MC, Alloosh M, Vuchetich JP, Mokelke EA, Sturek M. Components of metabolic syndrome and coronary artery disease in female ossabaw swine fed excess atherogenic diet. Comp Med. 2006; 56:35–45. [PubMed: 16521858]
18. Li Z, Woollard JR, Wang S, Korsmo MJ, Ebrahimi B, Grande JP, Textor SC, Lerman A, Lerman LO. Increased glomerular filtration rate in early metabolic syndrome is associated with renal adiposity and microvascular proliferation. Am J Physiol Renal Physiol. 2011; 301:F1078–F1087. [PubMed: 21775485]
19. Galili O, Versari D, Sattler KJ, Olson ML, Mannheim D, McConnell JP, Chade AR, Lerman LO, Lerman A. Early experimental obesity is associated with coronary endothelial dysfunction and oxidative stress. Am. J. Physiol.-Heart Circul. Physiol. 2007; 292:H904–H911.
20. Zhu XY, Daghini E, Chade AR, Napoli C, Ritman EL, Lerman A, Lerman LO. Simvastatin prevents coronary microvascular remodeling in renovascular hypertensive pigs. J Am Soc Nephrol. 2007; 18:1209–1217. [PubMed: 17344424]
21. Warner L, Glockner JF, Woollard J, Textor SC, Romero JC, Lerman LO. Determinations of renal cortical and medullary oxygenation using blood oxygen level-dependent magnetic resonance imaging and selective diuretics. Invest. Radiol. 2011; 46:41–47. [PubMed: 20856128]
22. Urbieta Caceres VH, Lin J, Zhu XY, Favreau FD, Gibson ME, Crane JA, Lerman A, Lerman LO. Early experimental hypertension preserves the myocardial microvasculature but aggravates cardiac injury distal to chronic coronary artery obstruction. Am. J. Physiol.-Heart Circul. Physiol. 2011; 300:H693–H701.
23. Zhu XY, Daghini E, Chade AR, Versari D, Krier JD, Textor KB, Lerman A, Lerman LO. Myocardial microvascular function during acute coronary artery stenosis: Effect of hypertension and hypercholesterolaemia. Cardiovasc. Res. 2009; 83:371–380. [PubMed: 19423617]
24. Rodriguez-Porcel M, Lerman A, Ritman EL, Wilson SH, Best PJM, Lerman LO. Altered myocardial microvascular 3D architecture in experimental hypercholesterolemia. Circulation. 2000; 102:2028–2030. [PubMed: 11044415]
25. Zhu XY, Rodriguez-Porcel M, Bentley MD, Chade AR, Sica V, Napoli C, Caplice N, Ritman EL, Lerman A, Lerman LO. Antioxidant intervention attenuates myocardial neovascularization in hypercholesterolemia. Circulation. 2004; 109:2109–2115. [PubMed: 15051643]
26. Kahn SE, Hull RL, Utzschneider KM. Mechanisms linking obesity to insulin resistance and type 2 diabetes. Nature. 2006; 444:840–846. [PubMed: 17167471]
27. Houstis N, Rosen ED, Lander ES. Reactive oxygen species have a causal role in multiple forms of insulin resistance. Nature. 2006; 440:944–948. [PubMed: 16612386]
28. Zhang XQ, Zhang RL, Raab S, Zheng W, Wang J, Liu N, Zhu TG, Xue LF, Song ZT, Mao JM, Li KT, Zhang HL, Zhang Y, Han C, Ding Y, Wang H, Hou N, Liu YL, Shang SJ, Li CY, Sebokova E, Cheng HP, Huang PL. Rhesus macaques develop metabolic syndrome with reversible vascular dysfunction responsive to pioglitazone. Circulation. 2011; 124 77-U176.
29. Lakhani M, Fein S. Effects of obesity and subsequent weight reduction on left ventricular function. Cardiol Rev. 2011; 19:1–4. [PubMed: 21135595]
30. Oliveira Junior SA, Dal Pai-Silva M, Martinez PF, Lima-Leopoldo AP, Campos DH, Leopoldo AS, Okoshi MP, Okoshi K, Padovani CR, Cicogna AC. Diet-induced obesity causes metabolic,

endocrine and cardiac alterations in spontaneously hypertensive rats. Med Sci Monit. 2010; 16:367–373.

31. Ruberg FL, Chen ZJ, Hua N, Bigornia S, Guo ZF, Hallock K, Jara H, LaValley M, Phinikaridou A, Qiao Y, Viereck J, Apovian CM, Hamilton JA. The relationship of ectopic lipid accumulation to cardiac and vascular function in obesity and metabolic syndrome. Obesity. 2010; 18:1116–1121. [PubMed: 19875992]
32. Glenn DJ, Wang F, Nishimoto M, Cruz MC, Uchida Y, Holleran WM, Zhang Y, Yeghiazarians Y, Gardner DG. A murine model of isolated cardiac steatosis leads to cardiomyopathy. Hypertension. 2011; 57 216-U175.
33. Zhang YM, Ren J. Role of cardiac steatosis and lipotoxicity in obesity cardiomyopathy. Hypertension. 2011; 57:148–150. [PubMed: 21220703]
34. Diamant M, Lamb HJ, Groeneveld Y, Endert EL, Smit JWA, Bax JJ, Romijn JA, de Roos A, Radder JK. Diastolic dysfunction is associated with altered myocardial metabolism in asymptomatic normotensive patients with well-controlled type 2 diabetes mellitus. J. Am. Coll. Cardiol. 2003; 42:328–335. [PubMed: 12875772]
35. de Kreutzenberg SV, Ceolotto G, Papparella I, Bortoluzzi A, Semplicini A, Dalla Man C, Cobelli C, Fadini GP, Avogaro A. Downregulation of the longevity-associated protein sirtuin 1 in insulin resistance and metabolic syndrome: Potential biochemical mechanisms. Diabetes. 2010; 59:1006–1015. [PubMed: 20068143]
36. Liang HY, Ward WF. Pgc-1 alpha: A key regulator of energy metabolism. Adv. Physiol. Educ. 2006; 30:145–151. [PubMed: 17108241]
37. Witteles RM, Fowler MB. Insulin-resistant cardiomyopathy. J. Am. Coll. Cardiol. 2008; 51:93–102. [PubMed: 18191731]
38. Arany Z, He HM, Lin JD, Hoyer K, Handschin C, Toka O, Ahmad F, Matsui T, Chin S, Wu PH, Rybkin II, Shelton JM, Manieri M, Cinti S, Schoen FJ, Bassel-Duby R, Rosenzweig A, Ingwall JS, Spiegelman BM. Transcriptional coactivator PGC-1 alpha controls the energy state and contractile function of cardiac muscle. Cell Metab. 2005; 1:259–271. [PubMed: 16054070]
39. Guerrero-Ontiveros ML, Wallimann T. Creatine supplementation in health and disease. Effects of chronic creatine ingestion in vivo: Down-regulation of the expression of creatine transporter isoforms in skeletal muscle. Mol. Cell. Biochem. 1998; 184:427–437. [PubMed: 9746337]
40. Meigs JB, Rutter MK, Sullivan LM, Fox CS, D'Agostino RB, Wilson PWF. Impact of insulin resistance on risk of type 2 diabetes and cardiovascular disease in people with metabolic syndrome. Diabetes Care. 2007; 30:1219–1225. [PubMed: 17259468]
41. Swynghedauw B. Molecular mechanisms of myocardial remodeling. Physiol. Rev. 1999; 79:215–262. [PubMed: 9922372]
42. Zhu XY, Daghini E, Rodriguez-Porcel M, Chade AR, Napoli C, Lerman A, Lerman LO. Redox-sensitive myocardial remodeling and dysfunction in swine diet-induced experimental hypercholesterolemia. Atherosclerosis. 2007; 193:62–69. [PubMed: 16996066]
43. Sobel BE, Schneider DJ, Lee YH, Pratley RE. Insulin resistance increases PAI-1 in the heart. Biochem. Biophys. Res. Commun. 2006; 346:102–107. [PubMed: 16750510]
44. Iliescu R, Chade AR. Progressive renal vascular proliferation and injury in obese zucker rats. Microcirculation. 2010; 17:250–258. [PubMed: 20536738]
45. Ghosh HS, McBurney M, Robbins PD. Sirt1 negatively regulates the mammalian target of rapamycin. PLoS One. 2010; 5:e9199. [PubMed: 20169165]
46. Koga H, Kaushik S, Cuervo AM. Altered lipid content inhibits autophagic vesicular fusion. Faseb J. 2010; 24:3052–3065. [PubMed: 20375270]
47. Harris J, De Haro SA, Master SS, Keane J, Roberts EA, Delgado M, Deretic V. T helper 2 cytokines inhibit autophagic control of intracellular mycobacterium tuberculosis. Immunity. 2007; 27:505–517. [PubMed: 17892853]
48. Boya P, Gonzalez-Polo RA, Casares N, Perfettini JL, Dessen P, Larochette N, Metivier D, Meley D, Souquere S, Yoshimori T, Pierron G, Codogno P, Kroemer G. Inhibition of macroautophagy triggers apoptosis. Mol Cell Biol. 2005; 25:1025–1040. [PubMed: 15657430]

49. Derdak Z, Lang CH, Villegas KA, Tong M, Mark NM, de la Monte SM, Wands JR. Activation of p53 enhances apoptosis and insulin resistance in a rat model of alcoholic liver disease. J Hepatol. 2011; 54:164–172. [PubMed: 20961644]

50. Alkhouri N, Gornicka A, Berk MP, Thapaliya S, Dixon LJ, Kashyap S, Schauer PR, Feldstein AE. Adipocyte apoptosis, a link between obesity, insulin resistance, and hepatic steatosis. J Biol Chem. 2010; 285:3428–3438. [PubMed: 19940134]

51. Katare RG, Caporali A, Oikawa A, Meloni M, Emanueli C, Madeddu P. Vitamin B1 analog benfotiamine prevents diabetes-induced diastolic dysfunction and heart failure through Akt/Pim-1-mediated survival pathway. Circ.-Heart Fail. 2010; 3:294–305. [PubMed: 20107192]

52. Rajesh M, Mukhopadhyay P, Batkai S, Patel V, Saito K, Matsumoto S, Kashiwaya Y, Horvath B, Mukhopadhyay B, Becker L, Hasko G, Liaudet L, Wink DA, Veves A, Mechoulam R, Pacher P. Cannabidiol attenuates cardiac dysfunction, oxidative stress, fibrosis, and inflammatory and cell death signaling pathways in diabetic cardiomyopathy. J. Am. Coll. Cardiol. 2010; 56:2115–2125. [PubMed: 21144973]

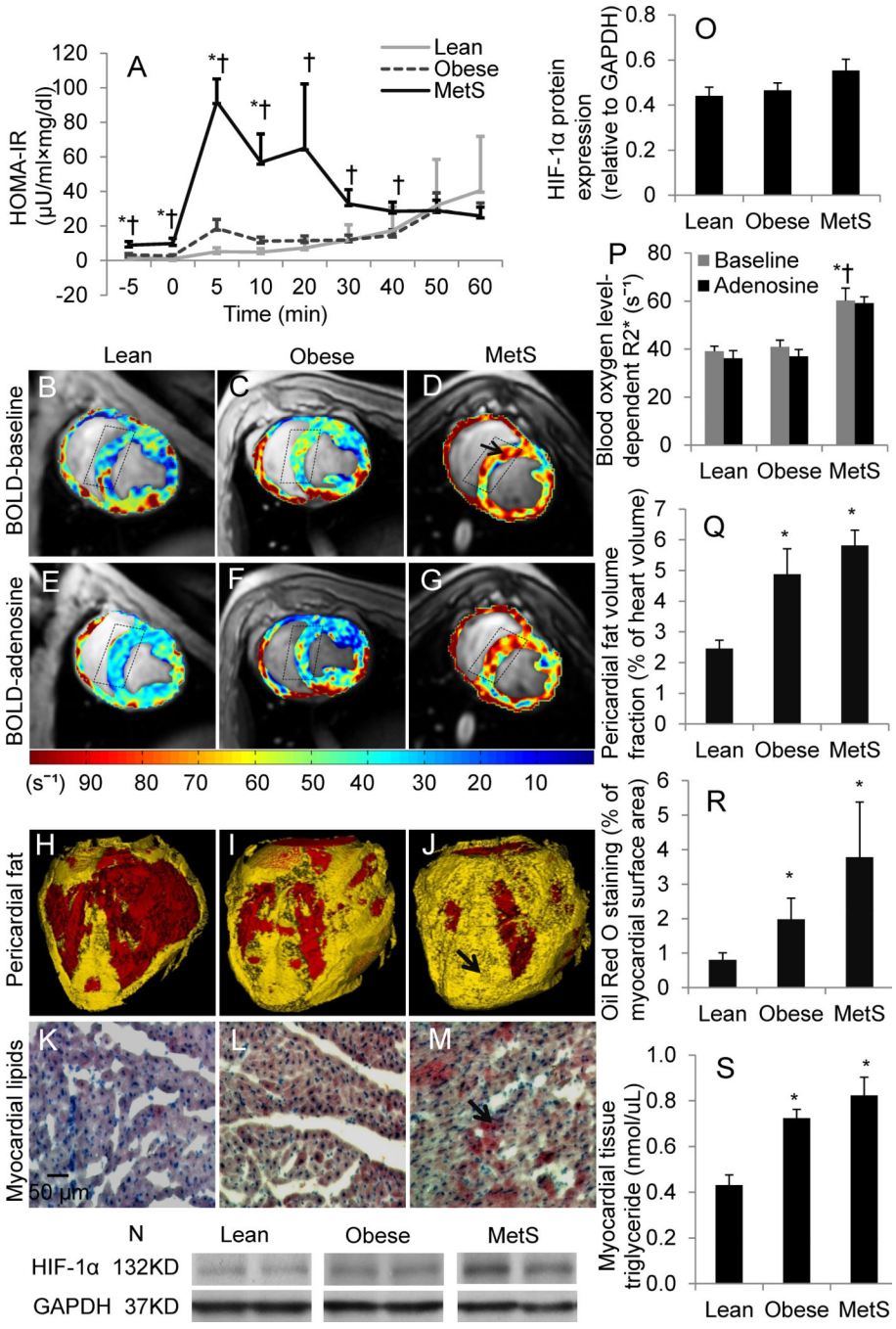

Figure 1.

Insulin resistance, myocardial oxygenation, and cardiac steatosis. Intravenous glucose tolerance tests (A). Representative cross-sectional images of Blood Oxygen Level-Dependent MRI (arrow indicates hypoxic myocardium) (B–G) and R_2* quantification (P); myocardial expression of hypoxia-inducible factor (HIF)-1α (N–O), which tended to increase in MetS compared with lean pigs. Representative three-dimensional CT images of pericardial fat (arrow) (H–J) and Oil-Red-O staining (red as arrow indicates) (K–M), and their quantifications (Q–R); levels of myocardial tissue triglyceride (S). HOMA-IR, homeostasis-model-assessment insulin resistance; MetS, metabolic syndrome. *$p \leq 0.05$ *vs.* lean, †$p \leq 0.05$ *vs.* obese. N=5 for Western-blot.

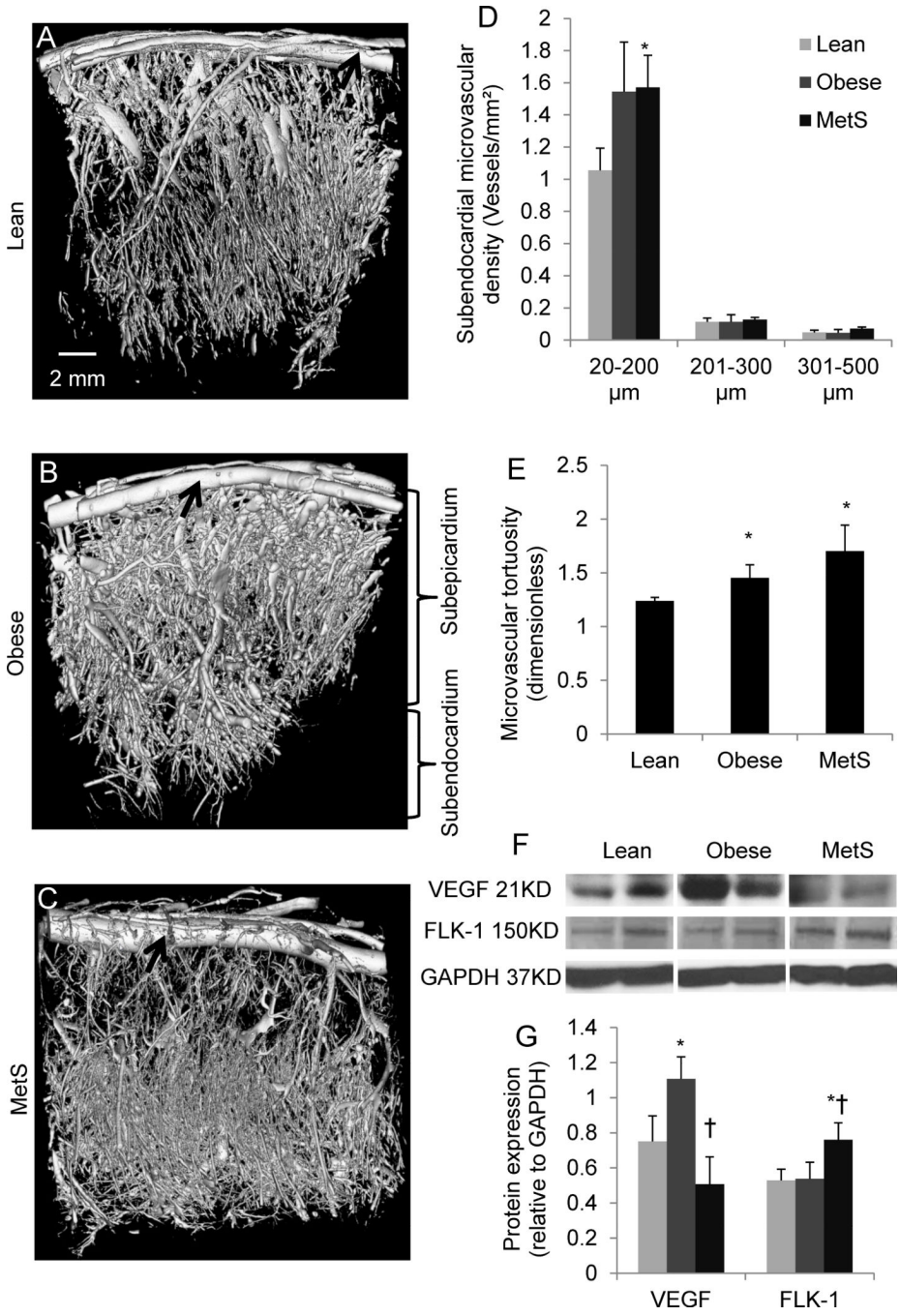

Figure 2.

Representative three-dimensional tomographic images of the myocardial microcirculation (A–C), subendocardial microvascular density quantification (D), and tortuosity (E); myocardial protein expression of vascular-endothelial growth-factor (VEGF) and its receptor FLK-1 (F), and their quantifications (G). *$p \leq 0.05$ *vs.* lean, †$p \leq 0.05$ *vs.* obese. Black arrows indicate epicardial arteries. N=5 for Western-blot.

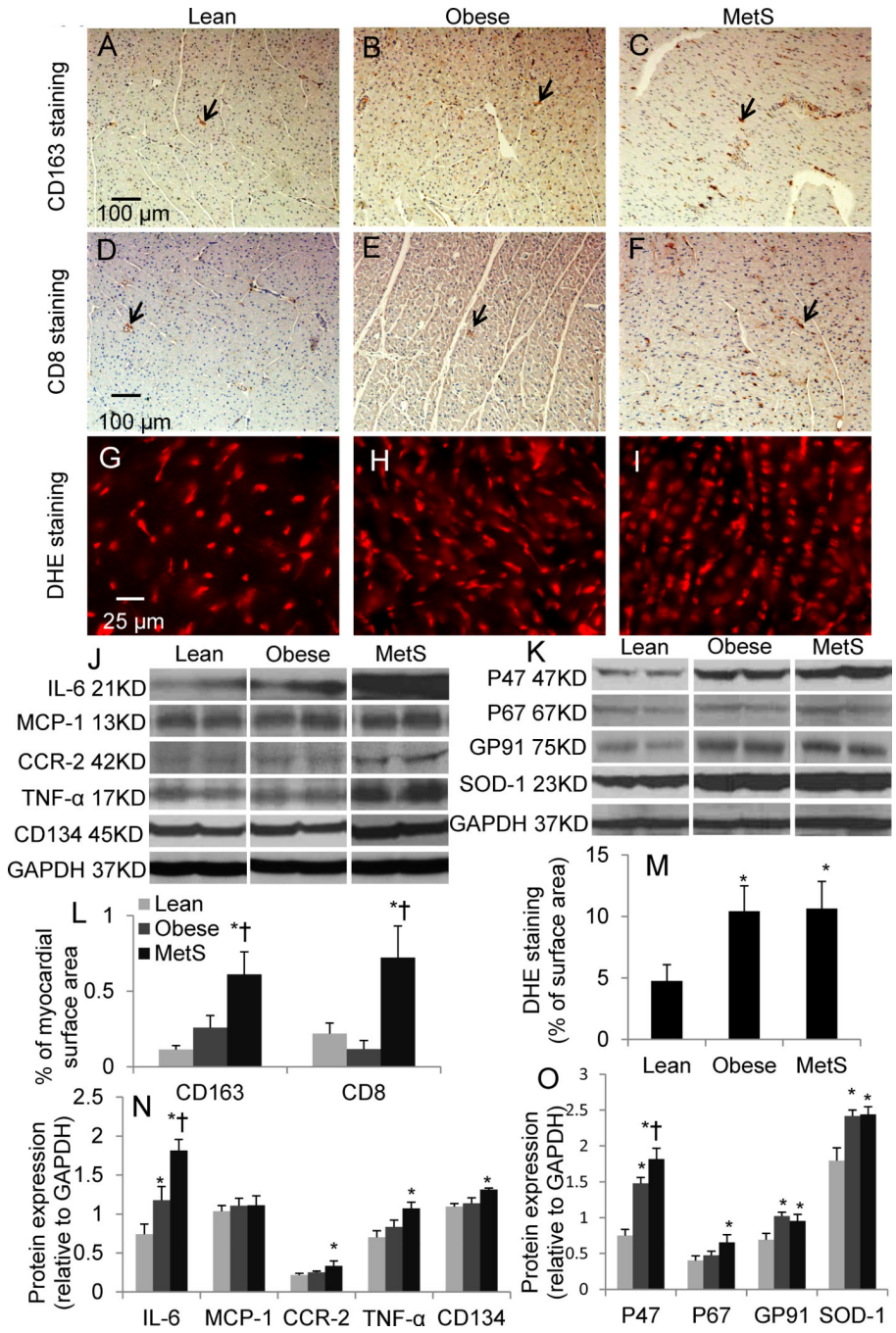

Figure 3.

CD163 (A–C), CD8 (D–F), and Dihydroethidium (DHE) (G–I) staining and quantifications (L–M); myocardial protein expression of inflammatory mediators (J) including interleukin (IL)-6, monocyte chemoattractant protein (MCP)-1), CCR-2, tumor necrosis factor-α (TNF-α), CD134, interferon (IFN)-γ, and oxidative stress markers (K) including P47, P67, GP91, and superoxide dismutase (SOD)-1, and their quantifications (N–O). $p \leq 0.05$ *vs.* lean, †$p \leq 0.05$ *vs.* obese. Black arrows indicate positive cells. N=6 for staining, N=5 for Western-blot.

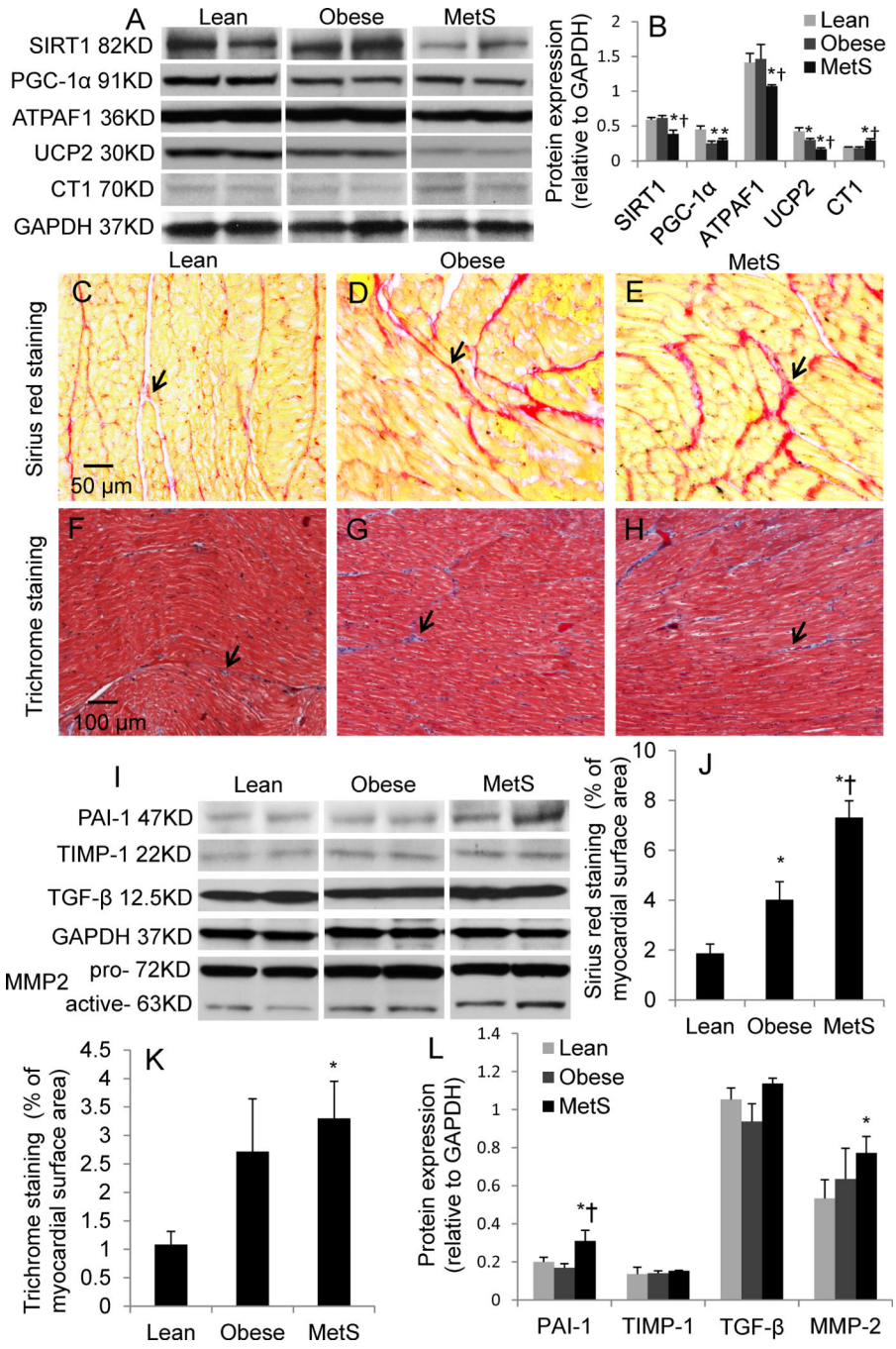

Figure 4.

Mitochondrial biogenesis, energy metabolism, and fibrosis. Myocardial protein expression of sirtuin 1 (SIRT1), peroxisome proliferator-activated receptor gamma coactivator 1-α (PGC-1α), ATP synthase mitochondrial F1 complex assembly factor 1 (ATPAF1), uncoupling protein-2 (UCP2), and creatine transporter 1 (CT1) and their quantification (A–B). Sirius red (C–E) and Trichrome (F–H) staining and quantifications (J–-K); myocardial protein expression of the fibrogenic factors (I) plasminogen-activator-inhibitor (PAI)-1, tissue-inhibitor of metalloproteinase (TIMP)-1, transforming growth-factor (TGF)-β1, and matrix metalloproteinase (MMP)-2, and their quantifications (L). $p \leq 0.05$ *vs.* lean, †$p \leq 0.05$

vs. obese. Black arrows indicate collagen in Sirius red and fiber in Trichrome staining, respectively. N=6 for staining, N=5 for Western-blot.

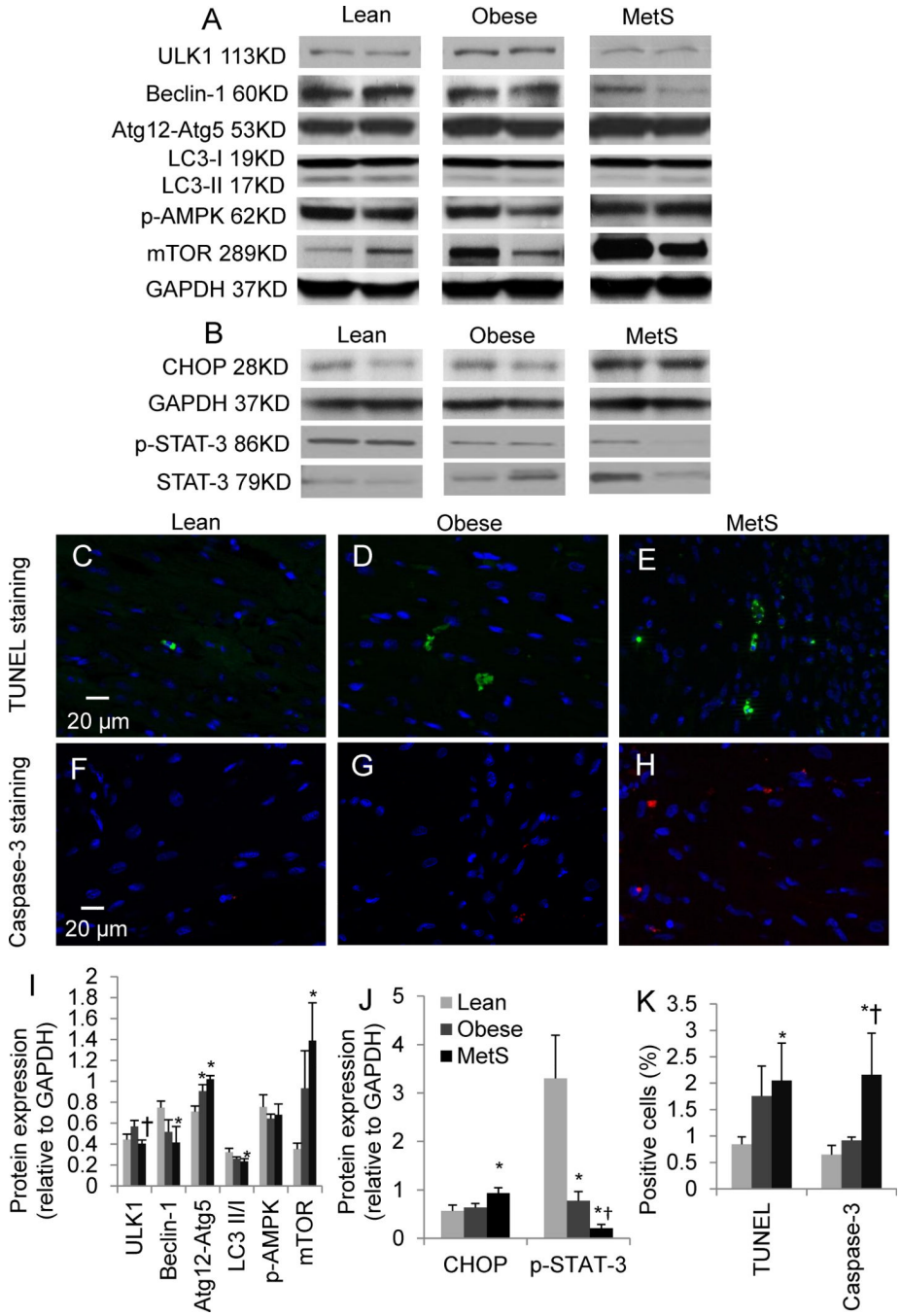

Figure 5.

Myocardial expression of autophagy-related proteins (A) including expression of unc-51-like kinase-1 (ULK1), Beclin-1, conjugated autophagy-related gene (Atg)12-Atg5, microtubule-associated protein-1 light chain 3 (LC3), phospho-AMP-activated protein kinase (p-AMPK), and mammalian target of rapamycin (mTOR), and apoptosis-related proteins (B) including CHOP and phosphorylated STAT-3, and their quantifications (I–J). Representative images of TUNEL (C–E), and Caspase-3 (F–H) staining, and their quantifications (K); $p \leq 0.05$ *vs.* lean, †$p \leq 0.05$ *vs.* obese. N=6 for staining, N=5 for Western-blot.

Table 1

Characteristics (*mean±SEM*) of lean, obese, and metabolic syndrome (MetS) pigs.

	Lean (n=6)	Obese (n=6)	MetS (n=6)
Body weight (kg)	16.6±2.1	24.1±2.2*	33.6±1.1*†
Intra-abdominal fat (%)	9.6±2.0	20.0±1.7*	32.3±3.4*†
Cholesterol (mg/dl): Total	79.8±6.5	364.8±90.6*	300.2±61.8*
Low-density lipoprotein	36.0±3.0	258.0±75.1*	193.7±34.7*
High-density lipoprotein	39.4±4.6	100.8±25.2*	97.8±29.6*
LDL/HDL	1.0±0.1	2.5±0.6*	2.5±0.5*
Plasma triglycerides (mg/dl)	22.0±5.7	29.8±8.2	43.4±13.7
Insulin (μU/ml)	0.1±0.05	0.4±0.1	0.9±0.2*†
Glucose (mg/dl)	132.3±54.9	132.4±17.1	231.3±26.5†
Oxidized low-density lipoprotein (ng/ml)	319.5±41.2	620.7±237.8	709.3±199.4*
8-epi-Isoprostane (pg/ml)	175.8±27.0	406.4±33.2*	551.0±124.2*
E/A	1.2±0.09	2.0±0.2*	2.3±0.3*
Mean arterial pressure (mmHg)	115.7±10.1	108.0±11.1	101.3±10.0
Heart rate (bpm)	63.6±8.3	73.3±10.2	74.4±9.2
Rate-pressure product (mmHg·bpm)	99.0±10.8	102.8±13.5	100.2±13.3
Stroke volume (ml)	26.1±2.0	28.8±1.5	33.7±3.3*
Cardiac output (L/min)	1.7±0.3	2.1±0.3	2.7±0.3*
Cardiac index (L/min/m^2)	4.1±0.6	3.8±0.6	3.8±0.3
Ejection fraction (%)	57.1±4.6	60.0±3.4	69.1±1.8*†
Permeability index (arbitrary units)			
Baseline	1.4±0.2	1.6±0.2	1.4±0.1
Adenosine	1.6±0.2	1.8±0.3	2.0±0.2§
Myocardial perfusion (ml/min/g)			
Baseline	0.9±0.07	1.0±0.07	1.2±0.2*
Adenosine	1.1±0.1§	1.1±0.05	1.3±0.2
Change after adenosine (%)	26.0±7.2	7.0±8.3	5.5±5.3*

*p≤0.05 vs. lean,

†p≤0.05 vs. obese,

§p≤0.05 vs. baseline.